On the Performance of Ultra-Wide-Band Signals in Gaussian Noise and Dense Multipath

Fernando Ramírez-Mireles, *Member, IEEE*

***Abstract*—An ultra-wide-band (UWB) signal is characterized by a radiated spectrum with a very wide bandwidth around a relatively low center frequency. In this paper, we study the reduced fading margin property of UWB signals. To evaluate the fading margin, we compare the performance of UWB signals in an environment with only additive white Gaussian noise (AWGN) versus the performance of UWB signals in a dense multipath environment with AWGN. The assumption here is that the presence of multipath causes a small increase in the signal-to-noise ratio required to achieve reasonable levels of bit error rate. A numerical example confirms this assumption. More specifically, the example shows that to achieve a bit error rate equal to 10^{-5}, we require about 13.5 dB in the AWGN case and about 15 dB in the multipath case, resulting in a fading margin of just 1.5 dB. This small fading margin can be understood by the ability of the UWB signal to resolve the dense multipath.**

***Index Terms*—Communication, multipath channels.**

I. Introduction

An ultra-wide-band (UWB) signal is characterized by a radiated spectrum with a very wide bandwidth around a relatively low center frequency. Typically, an UWB signal is defined as any signal in which the 3-dB bandwidth of the signal is at least 25% of its center frequency [1]. The wide bandwidth allows the signal to be received with fine time resolution, and a low enough center frequency allows the UWB signal to penetrate many materials. These two properties are relevant for communications in radio channels impaired with dense multipath, such as the wireless indoor channel [2]. With UWB signals, the dense multipath can be resolved, allowing the use of a Rake receiver [3] for signal demodulation. Therefore, the radio links can be operated in indoor environments with low-power transmission and with reduced fading margin, making UWB systems good candidates for short-range high-speed indoor wireless communications.[1]

In this paper, we are interested in the reduced fading margin property of UWB signals. The fading margin is the increase in required signal power to provide the same average error probability on fading versus nonfading channels [6]. The fading margin of UWB signals is studied by analyzing the performance of UWB signals for two cases: free-space propagation conditions with additive white Gaussian noise (AWGN case) and a dense multipath channel with AWGN (MP case).[2] The UWB signals considered here are based on subnanosecond pulses, which are generated relatively easily using current technology [1], [4].

We first describe the relation between the transmitted and received pulses. In the AWGN case, the transmitted pulse and the received UWB pulse are related by a mathematical operation. In the MP case, the transmitted pulse and the received dispersed UWB pulse is described using an ensemble of channel pulse responses. We also define the correlation properties of the received UWB in both cases.

Second, we define a set of UWB M-ary communication waveforms as pulse position modulated (PPM) signals consisting of more than one UWB pulse. We use PPM because it is straightforward to define M-ary waveforms in terms of the UWB pulses. In the MP case, we make the assumption that the multipath channel varies slowly with respect to the symbol waveform. The M-ary PPM signals are defined to be equally correlated in order to simplify the bit error rate (BER) analysis.

Third, we analyze the BER performance for an M-ary correlation receiver or matched filter. In the MP case, the BER is averaged over the energy and correlation variations caused by multipath in a particular wireless indoor channel.

Finally, numerical examples based on one particular UWB pulse are given. We use this particular UWB pulse because it has been used in previous studies of UWB communications [4], [7], [9].[3] These numerical examples are used to get a rough estimate of how much degradation in the average signal-to-noise ratio (SNR) is experienced using UWB signals in dense multipath channels.

II. Performance in Gaussian Noise

In this section, we analyze the performance of UWB signals under free-space propagation conditions with AWGN. We assume that both the transmitter and receiver are placed at certain fixed locations.

A. Channel Description and Signal Properties

The transmitted pulse is $p_{\mathrm{TX}}(t) \triangleq \int_{-\infty}^{t} p(\xi)\, d\xi$, and the received signal is $p(t)+n(t)$ (we ignore attenuation and delay due

Manuscript received December 7, 1999; revised September 26, 2000. This work was supported in part by the Joint Services Electronics Program under Contract F49620-94-0022.

The author was with the Electrical Engineering Department, University of Southern California, Los Angeles, CA 90007 USA. He is now with Aware Inc., Strategic Technologies Group, Lafayette, CA 94549 USA (e-mail: ramirezm@ieee.org).

Publisher Item Identifier S 0018-9545(01)01922-3.

[1]Although the UWB signals must contend with numerous narrow-band waveforms within their bandwidth, the technical feasibility of UWB communications has already been demonstrated [4], [5].

[2]For performance of UWB signals in a multiple access environment with AWGN, see [4], [7], and [8].

[3]Two on-line places that provide current information on UWB technology are USC's Ultra Lab (http://ultra.usc.edu/ulab) and Aether Wire (www.aether-wire.com).

to propagation). The effect of the antenna system in the transmitted pulse is modeled as a differentiation operation. The noise $n(t)$ is AWGN with two-sided power density $N_o/2$.

The UWB pulse $p(t)$ has duration T_p and energy $E_p = \int_{-\infty}^{\infty} [p(t)]^2\, dt$. The normalized signal correlation function of $p(t)$ is

$$\gamma_p(\tau) \triangleq \frac{1}{E_p} \int_{-\infty}^{\infty} p(t)p(t-\tau)\, dt > -1 \quad \forall \tau. \tag{1}$$

We define $\gamma_{\min} \triangleq \gamma_p(\tau_{\min})$ as the minimum value of $\gamma_p(\tau)$, $\tau \in (0, T_p]$.

Once we know the effect of the channel on a single pulse, we can describe the effect of the channel on the information signals. The transmitted signals are a kind of PPM signal, each composed of N_s time-shifted pulses

$$\Psi_{\mathrm{TX}}^{(j)}(t) = \sum_{k=0}^{N_s-1} p_{\mathrm{TX}}(t - kT_f - a_j^k \tau_{\min}) \tag{2}$$

$j = 1, 2, \ldots, M$. In the absence of noise, the received signals are composed of N_s time-shifted UWB pulses

$$\Psi_j(t) = \sum_{k=0}^{N_s-1} p(t - kT_f - a_j^k \tau_{\min}). \tag{3}$$

To analyze the performance of the signals in AWGN, we must describe the correlation properties of the *received* signals $\Psi_j(t)$ in (3). Each $\Psi_j(t)$ represents the jth signal in an ensemble of M signals, each signal completely identified by the sequence of time shifts $a_j^k \tau_{\min} \in \{0, \tau_{\min}\}$ (this choice of time shifts allows us to produce M-ary PPM signals, which are equally correlated). The a_j^k is a 0, 1 pattern representing the jth cyclic shift of an m-sequence of length N_s. Since there are at most N_s cyclic shifts in an m-sequence, we require that $2 \le M < N_s$. For a discussion of the properties of m-sequences and the requirements on the value of N_s, the reader is referred to [10]. We assume that the pulse duration satisfies $T_p + \tau_{\min} < T_f$, where T_f is the time shift value corresponding to the frame period. Each signal $\Psi_j(t)$ has duration $T_s \triangleq N_s T_f$ and energy $E_\Psi = N_s E_p$. The signals in (3) have normalized correlation values [11]

$$\beta_{ij} \triangleq \frac{\int_{-\infty}^{\infty} \Psi_i(t)\Psi_j(t)\, dt}{E_\Psi} = \beta = \frac{1+\gamma_{\min}}{2} \tag{4}$$

for all $i \neq j$, i.e., they are equally correlated.

B. Receiver and Bit Error Rate Performance

The optimum receiver is a bank of filters matched to the M signals $\Psi_j(t)$, $j = 1, 2, \ldots, M$. The receiver is assumed to be perfectly synchronized with the transmitter.

The union bound on the bit error probability using these equally correlated signals can be written [12]

$$\begin{aligned} \mathrm{UBPb} &= \frac{1}{M} \sum_{\substack{i=1 \\ i\neq j}}^{M} \sum_{j=1}^{M} Q\left(\sqrt{\frac{E_\Psi}{N_o}(1-\beta)}\right) \\ &= \frac{M}{2} \int_{\sqrt{\log_2(M)\mathbf{SNRb}}}^{\infty} \frac{\exp(-\xi^2/2)}{\sqrt{2\pi}}\, d\xi \end{aligned} \tag{5}$$

where

$$\mathbf{SNRb} = \frac{1}{\log_2(M)} \frac{E_\Psi}{N_o} (1-\beta) \tag{6}$$

is the received bit SNR and $Q(\xi)$ is the Gaussian tail function.

III. Numerical Example

To evaluate UBPb in (5) we need to calculate SNRb in (6). For this purpose, we need to know β in (4), i.e., we need to define the pulse $p(t)$ and the parameter $\tau_{\min}$ that define the signal in (3).

For $p(t)$, we consider a UWB pulse that can be modeled by the second derivative of a Gaussian function $\exp(-2\pi[t/t_n]^2)$ properly scaled. In this case, the transmitted pulse is

$$p_{\mathrm{TX}}(t) = t \exp\left(-2\pi \left[\frac{t}{t_n}\right]^2\right)$$

and the received pulse is

$$p(t) = \left[1 - 4\pi \left[\frac{t}{t_n}\right]^2\right] \exp\left(-2\pi \left[\frac{t}{t_n}\right]^2\right)$$

where the value $t_n = 0.7531$ ns was used to fit the model $p(t)$ to a measured waveform $p_m(t)$ from a particular experimental radio link [13]. This resulted in $T_p \simeq 2.0$ ns. The normalized signal correlation function corresponding to $p(t)$ is calculated using (1) to give

$$\gamma_p(t) = \left[1 - 4\pi \left[\frac{t}{t_n}\right]^2 + \frac{4\pi^2}{3} \left[\frac{t}{t_n}\right]^4\right] \exp\left(-\pi \left[\frac{t}{t_n}\right]^2\right).$$

For this $\gamma_p(t)$, we have $\tau_{\min} = 0.4073$ ns and $\gamma_{\min} = -0.6183$, so $\beta = 0.1909$ in (4). Both $p(t - T_p/2)$ and $\gamma_p(\tau)$ are depicted in Fig. 1. Fig. 2 shows the spectrum of the impulse $p(t)$. The 3-dB bandwidth of the pulse is close to 1 GHz. The center frequency is around 1.1 GHz.

Note that the specific value of N_s and T_f does not affect SNRb, as long as $M < N_s$ and $T_p + \tau_{\min} < T_f$. Hence, we set arbitrarily $T_f = 500$ ns and $N_s > 1000$.

The BER in AWGN can now be calculated using UBPb in (5). Results for different values of M are shown in Fig. 3. Values as large as $M = 128$ are easily obtained with the PPM signal design in (3), allowing us to exploit the benefits of M-ary modulation without an excessive increase in the complexity of the receiver [11].

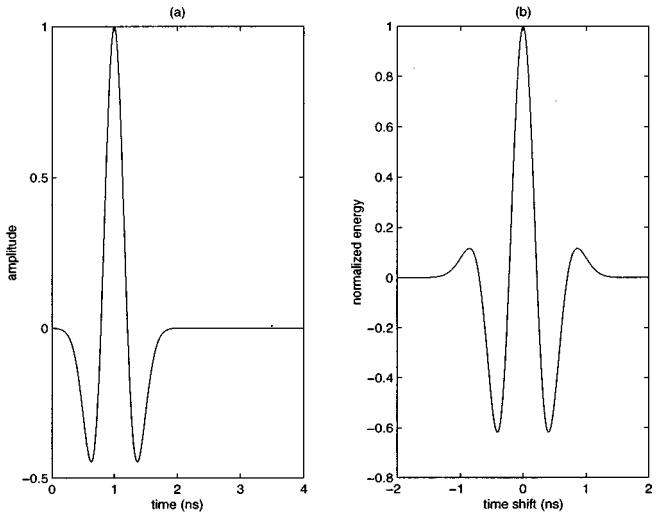

Fig. 1. (a) The pulse $p(t-(T_p/2))$ as a function of time $0 \le t \le 4$ ns. (b) The signal autocorrelation $\gamma_p(\tau)$ as a function of time shift $-2 \le \tau \le 2$ ns.

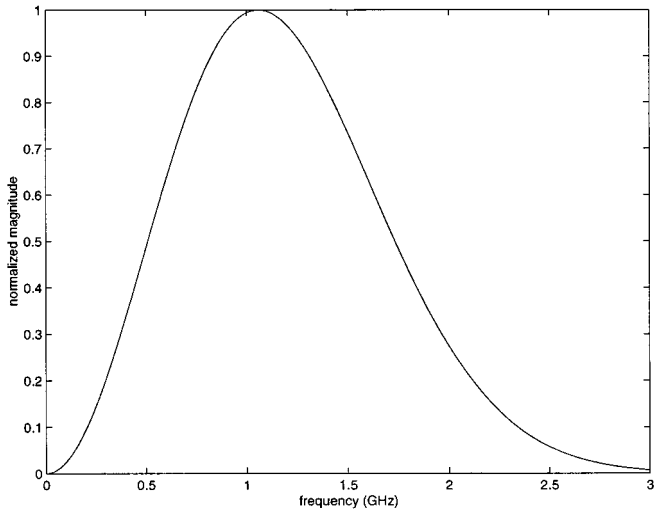

Fig. 2. The magnitude of the spectrum of the pulse $p(t)$.

Notice that the performance in AWGN depends on the correlation properties of the UWB signals and not on the UWB nature of the signals. In fact, any other set with the same M-ary correlation properties would give the same performance.

IV. Performance in Dense Multipath

In this section, we analyze the performance of UWB signals in a dense multipath channel with AWGN. The channel can be, for example, an indoor radio channel. In the analysis, we will assume that the transmitter is placed at a certain fixed location, and the receiver is placed at a variable location denoted u_o.

A. Channel Description and Signal Properties

The transmitted pulse is the same pulse $p_{\mathrm{TX}}(t)$ as in the AWGN case, and the received UWB signal is $\sqrt{E_a}\,\tilde{p}(u_o, t) + n(t)$. The pulse $\sqrt{E_a}\,\tilde{p}(u_o, t)$ is a multipath spread version of $p(t)$ received at position u_o with average duration $T_a \gg T_p$.

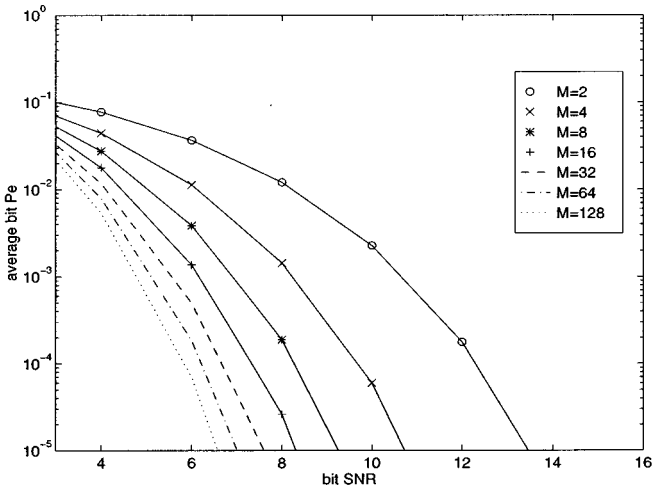

Fig. 3. The UBPb in (5). Curves for M are 2, 4, 8, 16, 32, 64, and 128 signals.

The pulse has "random" energy $\tilde{E}(u_o) \triangleq E_a\tilde{\alpha}^2(u_o)$, where E_a is the average energy and

$$\tilde{\alpha}^2(u_o) \triangleq \int_{-\infty}^{\infty} [\tilde{p}(u_o, t)]^2\, dt \tag{7}$$

is the normalized energy. The pulse has normalized signal correlation

$$\tilde{\gamma}(u_o, \tau) \triangleq \frac{\displaystyle\int_{-\infty}^{\infty} \tilde{p}(u_o, t)\tilde{p}(u_o, t-\tau)\, dt}{\displaystyle\int_{-\infty}^{\infty} [\tilde{p}(u_o, t)]^2\, dt}. \tag{8}$$

The transmitted information signals are the same $\Psi_{\mathrm{TX}}^{(j)}(t)$ as in the AWGN case given in (2). In the absence of noise, the received signals are composed of N_s time-shifted UWB pulses[4]

$$\tilde{\Psi}_j(u_o, t) = \sum_{k=0}^{N_s-1} \sqrt{E_a}\,\tilde{p}(u_o, t - kT_f - a_j^k\tau_{\min}) \tag{9}$$

for $j = 1, 2, \ldots, M$.

The UWB PPM signal $\tilde{\Psi}_j(u_o, t)$ is a multipath spread version of $\Psi_j(t)$ received at position u_o. We will assume that $\tilde{\Psi}_j(u_o, t)$ has fixed duration $T_s \simeq N_sT_f$, provided that $T_a + \tau_{\min} < T_f$. The signals in (9) have "random" energy

$$\begin{aligned}\tilde{E}_\Psi(u_o) &= \int_{-\infty}^{\infty} \left[\tilde{\Psi}_j(u_o, \xi)\right]^2 d\xi \\ &\simeq \overline{E}_\Psi\tilde{\alpha}(u_o)\end{aligned} \tag{10}$$

$j = 1, 2, \ldots, M$, where $\overline{E}_\Psi = N_sE_a$ is the average energy. The signals in (9) have normalized correlation values

$$\begin{aligned}\tilde{\beta}_{ij}(u_o) &\triangleq \frac{\displaystyle\int_{-\infty}^{\infty} \tilde{\Psi}_i(u_o, \xi)\tilde{\Psi}_j(u_o, \xi)\, d\xi}{\tilde{E}_\Psi(u_o)} \\ &= \tilde{\beta}(u_o) = \frac{1 + \tilde{\gamma}(u_o, \tau_{\min})}{2}\end{aligned} \tag{11}$$

for all $i \neq j$, i.e., they are equally correlated.

[4]The assumption that the multipath channel varies slowly with respect to the duration of the symbol waveform allows to assume that the M-ary PPM signal in (9) is composed of shifted replicas of the "same" multipath spread UWB pulse.

Obviously, the multipath effects change with the particular position u_o, and therefore the M-ary set of received signals $\{\tilde{\Psi}_j(u_o, t)\}_{j=1}^{j=M}$ also changes with that particular position u_o.

B. Receiver and Bit Error Rate Performance

Conditioned on a particular physical location u_o, the optimum receiver (matched filter) is a kind of perfect Rake receiver that is able to construct a reference signal $\tilde{\Psi}_j(u_0, T_s - t)$ that is perfectly matched to the signal received $\tilde{\Psi}_j(u_0, t)$ over the multipath conditions at that location u_0. We will assume that the receiver is perfectly synchronized with the transmitter.

Performance analysis for the perfect Rake receiver can be calculated using standard techniques [12]. Conditioned on a particular physical location u_o, the union bound on the bit error probability using these equally correlated signals can be written

$$\text{UBPb}(u_o) = \frac{M}{2} \int_{\sqrt{\log_2(M)\mathbf{SNRb}(u_o)}}^{\infty} \frac{\exp(-\xi^2/2)}{\sqrt{2\pi}}\, d\xi \quad (12)$$

where

$$\begin{aligned}\mathbf{SNRb}(u_o) &= \frac{1}{\log_2(M)} \frac{\tilde{E}_\Psi(u_o)}{N_o}(1 - \tilde{\beta}(u_o)) \\ &= \frac{1}{\log_2(M)} \frac{\overline{E}_\Psi \tilde{\alpha}^2(u_o)}{N_o} \left(1 - \tilde{\beta}(u_o)\right) \quad (13)\end{aligned}$$

is the received bit SNR [14]. The $\tilde{\beta}(u_o)$ value accounts for changes in the correlation properties of the received signals. These changes in $\tilde{\beta}(u_o)$ translate into changes in the Euclidean distance between signals [12]. Therefore, the $(1-\tilde{\beta}(u_o))$ value accounts for energy variations at the output of the perfect matched filter due to distortions in the shape of the signal correlation function caused by multipath. The $\tilde{\alpha}^2(u_o)$ value accounts for variations in the received signal energy due to fading caused by multipath.[5]

The average performance can be obtained by taking the expected value $\mathbf{E}_u\{\cdot\}$ over all values of u_o

$$\overline{\text{UBPb}}\left(\frac{\overline{E}_\Psi}{N_o}\right) = \mathbf{E}_u\left\{\text{UBPb}(u)\right\} \quad (14)$$

where

$$\left(\frac{\overline{E}_\Psi}{N_o}\right) \triangleq \mathbf{E}_u\left\{\mathbf{SNRb}(u)\right\}$$

is the average received bit SNR.

This BER analysis provides a theoretical matched filter bound for the best performance attainable when the multipath channel is perfectly estimated.

C. Statistical Characterization

Evaluation of $\overline{\text{UBPb}}(\overline{E}_\Psi/N_o)$ in (14) requires precise statistical characterization of the channel.

In traditional narrow-band communications, this characterization is based on a channel model in which a multipath signal is represented as a superposition of a number of pulses, each pulse with a different amplitude, time delay, and phase [2]. This channel model does not quite apply for wide-band signal propagation since the multipath signal is a superposition of a number of pulses, each pulse with a different amplitude, time delay, phase, and frequency content [17]. In the UWB case, this effect is more notorious. Each resolvable component has different frequency content since a UWB pulse suffers frequency distortions as it propagates through walls and other obstacles (the higher frequencies are likely to be attenuated more than lower frequencies).

Instead of using a channel model, we can make our calculations based on the *received* waveforms properly characterized. This is possible since the expected value in (14) is taken with respect to the quantities $\tilde{\alpha}^2(u_o)$ and $\tilde{\beta}(u_o)$. We can calculate histograms of these quantities for a particular indoor channel environment and get a first approximation using the sample mean value

$$\overline{\text{UBPb}}\left(\frac{\overline{E}_\Psi}{N_o}\right) \approx \frac{1}{u_*} \sum_{u_o=1}^{u_*} \text{UBPb}(u_o). \quad (15)$$

Since we are not using a specific channel model, confidence limits cannot be established properly. However, this calculation represents a rough approximation to the performance of UWB signals in the presence of dense multipath in a particular indoor radio environment.[6]

The histograms for $\tilde{\alpha}^2(u_o)$ and $\tilde{\beta}(u_o)$ can be derived from their definitions in (7) and (11) using the ensemble of pulse responses

$$\{\tilde{p}(u_o, t)\},\ u_o = 1, 2, \ldots, u_* \quad (16)$$

taken in a measurement experiment in the multipath channel of interest.

V. Numerical Example

To evaluate $\overline{\text{UBPb}}(\overline{E}_\Psi/N_o)$ in (15), we need to calculate $\text{UBPb}(u_o)$ in (12) and $\mathbf{SNRb}(u_o)$ in (13) for $u_o = 1, 2, \ldots, u_*$. For this purpose, we need to know the product $\tilde{\alpha}^2(u_o) \times (1 - \tilde{\beta}(u_o))$, i.e., we need to describe the pulse $\tilde{p}(u_o, t)$ and the parameters that define the signals $\tilde{\Psi}_j(u_o, t)$ in (9).

Let the transmitted pulse be the same $p_{\text{TX}}(t)$ that was used in the numerical example for the AWGN-only case. For the multipath case, the received pulse is described by the ensemble in (16). This ensemble is formed with channel pulse responses $\tilde{p}(u_o, t)$ measured in a UWB propagation experiment [19]. This experiment is described in detail in [13] and is summarized in the Appendix of this paper.

A total of $u_* = 392$ channel pulse responses $\tilde{p}(u_o, t)$ were measured. An equal number of normalized energy values $\tilde{\alpha}^2(u_o)$ and normalized correlation functions $\tilde{\gamma}(u_o, \tau)$ were calculated using (7) and (8), respectively. One of the measured pulses $\tilde{p}(u_o, t)$ is depicted in Fig. 4. The normalized correlation function $\tilde{\gamma}(u_o, \tau)$ of the pulse in Fig. 4 is depicted in Fig. 5. Fig. 6 shows histograms of $\tilde{\alpha}^2(u_o)$, $\tilde{\beta}(u_o)$, and the product $\tilde{\alpha}^2(u_o) \times (1 - \tilde{\beta}(u_o))$.

[5]Previous analysis did not consider both sources of energy variation separately. For example, [15] analyzes UWB propagation from the perspective of variations in the received signal energy and [16] analyzes UWB propagation from the signal waveform distortion point of view.

[6]This method to calculate BER performance is similar to the quasi-analytical method in [18], except that the waveforms are not modeled analytically but measured in a real channel.

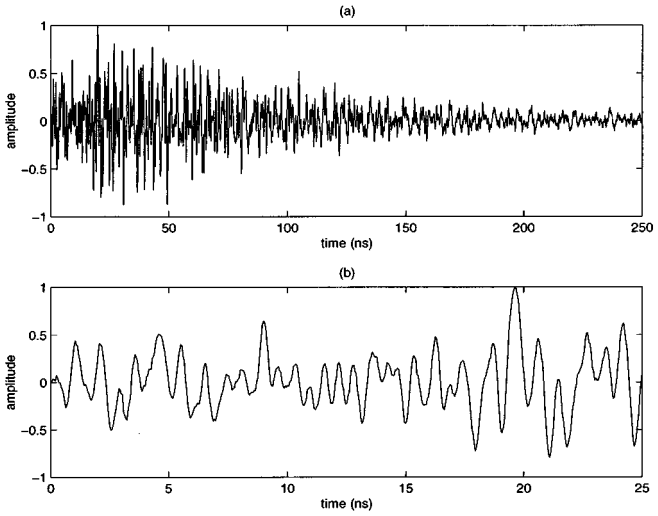

Fig. 4. (a) One of the measured pulses $\bar{p}(u_o,\, t)$ (normalized in amplitude). (b) A closer view of the pulse in (a). The spreading caused by multipath is notorious. The high multipath resolution of the UWB signal is evident.

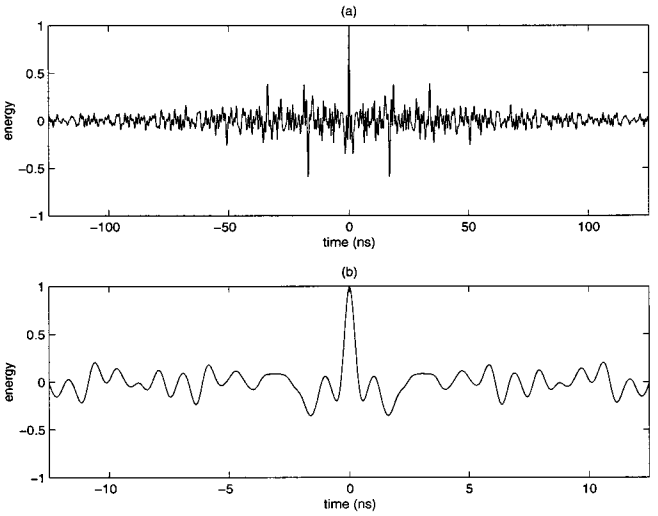

Fig. 5. (a) Normalized correlation function $\bar{\gamma}(u_o,\, \tau)$ of the pulse $\bar{p}(u_o,\, t)$ in Fig. 4. (b) A closer view of the correlation in (a). The long tails in the correlation function are the effect of the pulse spreading.

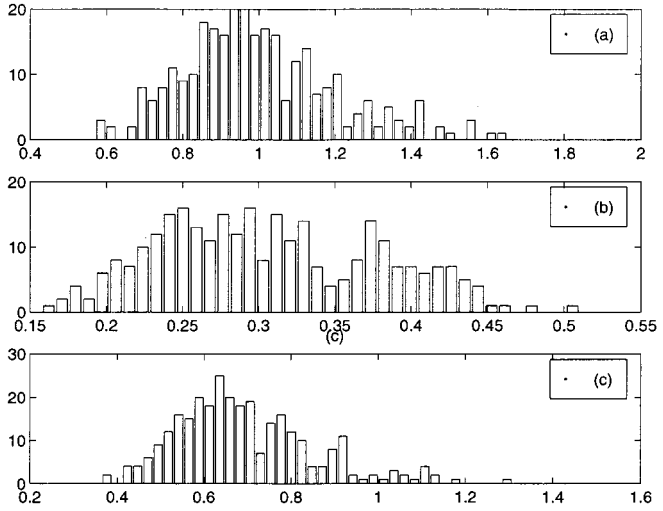

Fig. 6. The histograms of the normalized values of (a) the received energy $\bar{\alpha}^2(u)$, (b) the correlation value $\bar{\beta}(u)$, and (c) the product $\bar{\alpha}^2(u)[1-\bar{\beta}(u)]$. The ordinate represents appearance frequency, and the abscissa represents the value of the parameter. The size of the sample is $u_* = 392$.

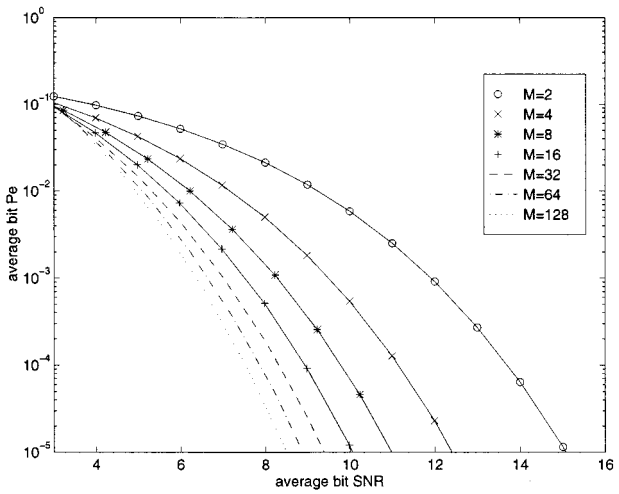

Fig. 7. The $\overline{\text{UBPb}}(\overline{E}_\Psi/N_o)$ in (15). Curves for $M = 2, 4, 8, 16, 32, 64$, and 128 signals.

The measured $\tilde{p}(u_o,\, t)$ have $T_a \simeq 300$ ns. The rest of the parameters values are the same as those used in the AWGN case, i.e., $\tau_{\min} = 0.4073$ ns, $T_f = 500$ ns, and $N_s > 1000$. With these values, the conditions $M < N_s$ and $T_a + \tau_{\min} < T_f$ will be satisfied.

We now can calculate numerical values for (13), (12), and (15). Fig. 7 shows the curves for $\overline{\text{UBPb}}(\overline{E}_\Psi/N_o)$ with M of 2, 4, 8, 16, 32, 64, and 128. Values as large as $M = 128$ are easily obtained with the PPM signal design in (9), allowing us to exploit the benefits of M-ary modulation.

VI. Conclusion

We calculated the performance of UWB signals both in a dense multipath environment with AWGN (Fig. 7) and in an environment with only AWGN (Fig. 3). As can be seen from the figures, the presence of multipath causes a small increase in the SNR required to achieve reasonable levels of BER. For example, to achieve BER equal to 10^{-5} with $M = 2$, we require about 13.5 dB in the AWGN case and about 15 dB in the multipath case, an extra SNR penalty of just 1.5 dB. The reason for this small SNR fading margin can be understood by the ability of the UWB signal to resolve the dense multipath.

In contrast, narrow-band modulations such as binary phase-shift keying in a Rayleigh fading environment require a fading margin of about 35 dB to achieve the same BER of 10^{-5} [6].

The reduced fading margin in the UWB signal is obtained at the expense of receiver complexity. Due to their ability to resolve the dense multipath, the UWB receiver is faced with the challenging task of "raking" the signal energy dispersed in the multiple paths.

The small fading margin for UWB signals calculated here using the "perfect Rake" receiver is, of course, an idealistic value representing a theoretical lower bound in performance. Since implementation restrictions in practical Rake receivers reduce the usefulness of taps beyond some limit, more study is needed to evaluate the impact of these restrictions on the performance of the system.

The sample average calculation made in this paper is a rough approximation to the performance of UWB signals in the presence of dense multipath in a particular indoor radio environment. Perhaps the major virtue of this method of calculation is that once the experimental data is processed, it can generate BER curves for different signal designs in just a few seconds. Thus, in the absence of great accuracy, we found the method useful for fading margin calculation based on comparative evaluations.

APPENDIX

This Appendix provides a brief description of the measurements experiment configuration and the data collection procedure.

The channel responses $\tilde{p}(u_o, t)$ were measured in eight different rooms and hallways in a typical office building. In every room and hallway, 49 different locations are arranged spatially in a 7×7 square grid with 6 in per side. At every location u_o, the $T_a = 300$ ns-long pulses $\tilde{p}(u_o, t)$ are recorded keeping the transmitter, the receiver, and the environment stationary.

The UWB transmitter is placed at a fixed location inside the building. It consists of a step recovery diode-based pulser connected to an UWB omnidirectional antenna. The pulser produces a train of UWB "Gaussian monocycles"[7] $p_{\mathrm{TX}}(t)$. The train of $p_{\mathrm{TX}}(t)$ is transmitted as an excitation signal to the propagation channel. The train has a repetition rate of 500 ns with a tightly controlled average monocycle-to-monocycle interval. The clock driving the pulser has resolution in the order of picoseconds.

The $\tilde{p}(u_o, t)$ represents the convolution of $p_{\mathrm{TX}}(t)$ with the channel impulse response at location u_o. The 500-ns repetition rate is long enough to make sure that pulse responses $\tilde{p}(u_o, t)$ corresponding to adjacent impulses $p_{\mathrm{TX}}(t)$ do not overlap.

The receiver consists of a UWB antenna and a low-noise amplifier. The output of this amplifier is captured using a high-speed digital sampling scope. The scope takes samples in windows of 50 ns at a sampling rate of 20.5 GHz. Noise in the measured $\tilde{p}(u_o, t)$ is reduced by averaging 32 consecutive received pulses measured at exactly the same location u_o. These samples are sent to a data storage and processing unit.

ACKNOWLEDGMENT

The author is very grateful to Dr. R. A. Scholtz for his guidance and advice during this research endeavor. He owes thanks to Dr. M. Z. Win for setting the experimental configuration and providing the UWB signal propagation data that the author used to elaborate the numerical example. He wants to thank Time Domain Inc. for providing the facilities to Dr. Win to carry on the experiment. He also wants to give special thanks to the anonymous reviewers whose comments helped to improve the quality of this paper.

REFERENCES

[1] J. D. Taylor, Ed., *An Introduction to Ultra Wideband Radar Technology*. Boca Raton, FL: CRC Press, 1995.
[2] H. Hashemi, "The indoor radio propagation channel," *Proc. IEEE*, vol. 81, no. 7, pp. 943–968, July 1993.
[3] R. Price and P. E. Green Jr., "A communication technique for multipath channels," *Proc. IRE*, pp. 555–570, Mar. 1958.
[4] P. Withington II and L. W. Fullerton, "An impulse radio communications system," in *Ultra-Wideband, Short-Pulse Electromagnetics*, H. L. Bertoni, L. Carin, and L. B. Felson, Eds. New York: Plenum, 1993, pp. 113–120.
[5] "Time domain radio transmission system," U.S. Patent 5 812 081, 1995.
[6] K. Pahlavan and A. H. Levesque, *Wireless Information Networks*. New York, NY: John Wiley and Sons, 1995, p. 241.
[7] R. A. Scholtz, "Multiple access with time hopping impulse modulation," in *Proc. IEEE MILCOM Conf.*, 1993, pp. 447–450.
[8] F. Ramírez-Mireles and R. A. Scholtz, "Multiple-access with time hopping and block waveform PPM modulation," in *Proc. IEEE ICC Conf.*, 1998, pp. 775–779.
[9] F. Ramírez-Mireles, "Multiple-access with ultra-wideband impulse radio modulation using spread spectrum time-hopping and block waveform pulse-position-modulated signals," Ph.D. dissertation, Communication Sciences Institute, Electrical Engineering Department, University of Southern California, 1998.
[10] S. W. Golomb, "Construction of signals with favorable correlation properties," in *Surveys in Combinatorics*. London, Mathematical Society Lecture Notes Series 166, U.K.: Cambridge Univ. Press, 1991.
[11] F. Ramírez-Mireles and R. A. Scholtz, "Time-shift-keyed equicorrelated signal sets for impulse radio M-ary modulation," in *Proc. IEEE WIRELESS Conf.*, 1998, pp. 404–408.
[12] R. M. Gagliardi, *Introduction to Telecommunications Engineering*. New York: Wiley, 1988, pp. 357–437.
[13] M. Z. Win, F. Ramírez-Mireles, R. A. Scholtz, and M. A. Barnes, "Ultra-wide bandwidth (UWB) signal propagation for outdoor wireless communications," in *Proc. IEEE VTC Conf.*, May 1997, pp. 251–255.
[14] F. Ramírez-Mireles and R. A. Scholtz, "Performance of equicorrelated ultra-wideband pulse-position-modulated signals in the indoor wireless impulse radio channel," in *Proc. IEEE PACRIM Conf.*, 1997, pp. 640–644.
[15] M. Z. Win and R. A. Scholtz, "On the energy capture of ultra-wide bandwidth signals in dense multipath environments," *IEEE Commun. Lett.*, vol. 2, pp. 245–247, Sept. 1998.
[16] R. C. Qiu, "A theoretical study of the ultra-wideband wireless propagation channel based on the scattering centers," Radio Science, submitted for publication.
[17] R. C. Qiu and I.-T. Lu, "Multipath resolving with frequency dependence for wide-band wireless channel modeling," *IEEE Trans. Veh. Technol.*, vol. 48, pp. 273–285, Jan. 1999.
[18] M. C. Jeruchim, "Techniques for estimating the bit error rate in the simulation of digital communication systems," *IEEE J. Select. Areas Commun.*, vol. 48, pp. 273–285, Jan. 1999.
[19] M. Z. Win and R. A. Scholtz, "Ultra-wide bandwidth (UWB) signal propagation for indoor wireless communications," in *Proc. IEEE ICC Conf.*, June 1997, pp. 56–60.

[7] A Gaussian monocycle is the first derivative of a Gaussian function.

Fernando Ramírez-Mireles (M'88) received the B.S.E.E. degree from the Metropolitan Autonomous University (UAM), Mèxico, the M.S.E.E. degree from the Center for Advanced Studies of IPN, Mèxico, and the Ph.D.E.E. degree from the University of Southern California (USC), Los Angeles.

He was with the Mexican Telephone Company and CINVESTAV. He consulted for the National Bank of Mexico. He was a Research Assistant with USC's Communication Sciences Institute, where he worked on ultra-wide-band (UWB) communications. In the summer of 1997, he was an MTS with Torrey Science Corporation, San Diego, CA, where he worked on spread-spectrum LEO satellite communications. From 1998 to 1999, he was an MTS with Glenayre Technologies, Santa Clara, CA, where he worked on definition of demodulation architectures for NPCS mobile terminals. Presently, he is an MTS with Aware, Inc., Lafayette, CA, working on technology development for current and future standards of DSL. He has published 16 technical articles in areas including modulation and signal design for UWB communications, spread-spectrum multiple-access performance, performance in multipath channels, and speech recognition. He has one U.S. patent pending on DSL.

Dr. Ramírez-Mireles is a member of Tau Beta Pi. He was a Fulbright Scholar while pursuing the Ph.D. degree. In Mèxico, he received Honorable Mention for the IV Ericsson National Prize of Science and Technology. He received the Medal to the Universitarian Merit.